



PERGAMON

International Journal of Solids and Structures 38 (2001) 5995–6014

INTERNATIONAL JOURNAL OF  
**SOLIDS and**  
**STRUCTURES**

[www.elsevier.com/locate/ijsolstr](http://www.elsevier.com/locate/ijsolstr)

## Ill-conditioning of finite element poroelasticity equations

Massimiliano Ferronato <sup>\*</sup>, Giuseppe Gambolati, Pietro Teatini

DMMSMA – Department of Mathematical Methods and Models for Scientific Applications, University of Padova, Via Belzoni 7,  
35131 Padova, Italy

Received 15 March 2000

---

### Abstract

The solution to Biot's coupled consolidation theory is usually addressed by the finite element (FE) method thus obtaining a system of first-order differential equations which is integrated by the use of an appropriate time marching scheme. For small values of the time step the resulting linear system may be severely ill-conditioned and hence the solution can prove quite difficult to achieve. Under such conditions efficient and robust projection solvers based on Krylov's subspaces which are usually recommended for non-symmetric large size problems can exhibit a very slow convergence rate or even fail. The present paper investigates the correlation between the ill-conditioning of FE poroelasticity equations and the time integration step  $\Delta t$ . An empirical relation is provided for a lower bound  $\Delta t_{\text{crit}}$  of  $\Delta t$  below which ill-conditioning may suddenly occur. The critical time step is larger for soft and low permeable porous media discretized on coarser grids. A limiting value for the rock stiffness is found such that for stiffer systems there is no ill-conditioning irrespective of  $\Delta t$  however small, as is also shown by several numerical examples. Finally, the definition of a different  $\Delta t_{\text{crit}}$  as suggested by other authors is reviewed and discussed. © 2001 Elsevier Science Ltd. All rights reserved.

**Keywords:** Finite elements; Coupled poroelasticity; Ill-conditioning; Critical time step; Convergence rate; Projective solvers

---

### 1. Introduction

The time-dependent distribution of displacement and fluid pore pressure in porous media was first mathematically described by Biot (1941). Biot's consolidation theory couples the elastic equilibrium equations with a continuity or mass balance equation which may be solved under appropriate boundary and initial flow and loading conditions.

The consolidation problem is usually solved in space by a finite element (FE) technique giving rise to a system of first-order differential equations. The solution to these equations is typically addressed by an appropriate time marching scheme. The discretization in the time domain may require variable time steps which may change by several orders of magnitude during the analysis. As a matter of fact, in the early phase

---

<sup>\*</sup>Corresponding author. Tel.: +39-049-8275929; fax: +39-049-8725995.

E-mail address: [ferronat@dmsa.unipd.it](mailto:ferronat@dmsa.unipd.it) (M. Ferronato).

of consolidation small time steps are needed to obtain a sufficiently accurate solution, while, as the simulation proceeds, a much larger time step can be used without a great loss of accuracy. Time integration is usually performed by the well-known  $\theta$ -method, whose stability and accuracy has been widely discussed by a number of authors (Booker and Small, 1975; Vermeer and Verruijt, 1981). In particular, Booker and Small (1975) proved that an implicit time integration scheme with  $\theta \geq 0.5$  is unconditionally stable even if the sequence of time steps  $\Delta t_i$  is strictly increasing, while the choice  $\theta < 0.5$  is conditionally stable and may require a very small time step.

Furthermore, the solution to the linear system with a small  $\Delta t$  may prove quite difficult, as was also observed by some authors (Ghaboussi and Wilson, 1973; Vermeer and Verruijt, 1981; Reed, 1984; Sloan and Abbo, 1999). The problems arising from the choice of a small time step were first noted by Ghaboussi and Wilson (1973) who suggest a criterion for a minimum  $\Delta t$  in order to prevent the global system from becoming ill-conditioned. They point out that ill-conditioning is related to the large difference between the terms arising from the integration of equilibrium equations and those from the flow equation. A practical way to avoid ill-conditioning is suggested by Reed (1984) by the use of a scaling factor to reduce the difference in magnitude of the pivotal elements. A suitable value for the scaling factor is provided by Sloan and Abbo (1999) who try to equate approximately the size of diagonal terms of the structural equations and those of the flow equation. One such scaling strategy was implemented in a code by Lewis and Schrefler (1987).

Although sophisticated direct sparse solvers (Duff et al., 1986) may prove quite efficient for unsymmetric, non-positive definite matrices, the large dimension of the linear systems generated by the FE method in realistic consolidation problems (and particularly so in those related to fluid withdrawal) suggests that iterative methods be used. In particular, projection methods based on Krylov's subspaces, such as biconjugate gradient stabilized (Bi-CGSTAB) and transpose free quasi-minimal residual (TFQMR) effectively preconditioned (Saad, 1996), prove quite efficient in the solution of large size problems (Gambolati et al., 1996). Unfortunately, the scaling strategy mentioned above, while probably giving good results with direct techniques, may appear to be inefficient when used with projection methods.

A deeper analysis of the correlation existing between the time step and the physical parameters describing the consolidation problem is offered by Vermeer and Verruijt (1981) who define a lower bound for  $\Delta t$  below which numerical oscillations in the solution may appear. This stability condition is based on the observation that the excess pore pressure due to an instantaneous load applied on a draining porous column cannot exceed the load itself.

In the present paper we investigate the numerical factors which may influence ill-conditioning of the linear systems arising from the FE integration of coupled poroelastic models. A simple argument is given to account for the inception of ill-conditioning vs. the size of  $\Delta t$  with the definition of a critical time step below which ill-conditioning suddenly occurs. We show that the concept of  $\Delta t_{\text{crit}}$  is basically related to the difficulty of finding the solution rather than to the accuracy of the solution itself, which may prove quite accurate also for time steps smaller than the critical  $\Delta t$  provided that one is willing to pay a sufficiently high computational cost. Finally, some numerical examples are given to substantiate the theoretical arguments.

## 2. Finite element formulation of Biot consolidation equations

According to Biot's (1941) formulation, as later modified by van der Knaap (1959) and Geertsma (1966), the coupled model for an isotropic medium reads:

$$(\lambda + G) \frac{\partial \epsilon}{\partial i} + G \nabla^2 u_i = \alpha \frac{\partial p}{\partial i} \quad i = x, y, z, \quad (1)$$

$$\frac{1}{\gamma} \nabla(k \nabla p) = [n\beta + c_{br}(\alpha - n)] \frac{\partial p}{\partial t} + \alpha \frac{\partial \epsilon}{\partial t}, \quad (2)$$

where  $c_{br}$  and  $\beta$  are the volumetric compressibility of solid grains and water, respectively;  $n$  is the porosity;  $k$  is the medium hydraulic conductivity;  $\epsilon$  is the medium volumetric dilatation;  $\alpha$  is the Biot coefficient;  $\lambda$  and  $G$  are the Lamé constant and the shear modulus of porous medium;  $\gamma$  is the specific weight of water;  $\nabla$  is the gradient operator;  $x$ ,  $y$ ,  $z$  are the coordinate directions and  $t$  is time;  $p$  and  $u_i$  are the incremental pore pressure and the components of incremental displacement along the  $i$ -direction, respectively.

The widely accepted assumption of rigid solid grains ( $c_{br} = 0$  and  $\alpha = 1$ ) (Verruijt, 1969) leads to a more familiar form of Eq. (2):

$$\frac{1}{\gamma} \nabla(k \nabla p) = n\beta \frac{\partial p}{\partial t} + \frac{\partial \epsilon}{\partial t}. \quad (3)$$

FE solutions to the coupled Eqs. (1) and (3) were originally developed by several authors (Sandhu and Wilson, 1969; Christian and Boehmer, 1970; Hwang et al., 1971; Desai, 1975; Sandhu, 1976; Smith and Hobbs, 1976; Verruijt, 1977). Integration in space yields a system of first-order differential equations which can be written as:

$$\begin{bmatrix} K & -Q \\ 0 & H \end{bmatrix} \begin{Bmatrix} \mathbf{u} \\ \mathbf{p} \end{Bmatrix} + \begin{bmatrix} 0 & 0 \\ Q^T & P \end{bmatrix} \begin{Bmatrix} \dot{\mathbf{u}} \\ \dot{\mathbf{p}} \end{Bmatrix} = \begin{Bmatrix} \mathbf{f}^u \\ \mathbf{f}^p \end{Bmatrix} \quad (4)$$

where  $K$ ,  $H$ ,  $P$  and  $Q$  are the elastic stiffness, flow stiffness, flow capacity and coupling matrices, respectively;  $\begin{Bmatrix} \mathbf{u} \\ \mathbf{p} \end{Bmatrix}$  and  $\begin{Bmatrix} \dot{\mathbf{u}} \\ \dot{\mathbf{p}} \end{Bmatrix}$  are the vector of the unknown variables  $u_i$  and  $p$  and corresponding time derivatives;  $\begin{Bmatrix} \mathbf{f}^u \\ \mathbf{f}^p \end{Bmatrix}$  is the vector for the nodal loads ( $\mathbf{f}^u$ ) and flow sources ( $\mathbf{f}^p$ ).

The explicit expressions of the above matrices are given in Appendix A.

Eq. (4) can be written in a more compact form as:

$$K_1 \mathbf{x} + K_2 \dot{\mathbf{x}} + \mathbf{f} = 0, \quad (5)$$

where the meaning of the symbols can be derived by a simple comparison between Eqs. (4) and (5). Applying the  $\theta$ -method marching scheme to solve Eq. (5) yields:

$$\left[ \theta K_1 + \frac{1}{\Delta t} K_2 \right] \mathbf{x}_{m+1} = \left[ \frac{1}{\Delta t} K_2 - (1 - \theta) K_1 \right] \mathbf{x}_m - [\theta \mathbf{f}_{m+1} + (1 - \theta) \mathbf{f}_m]. \quad (6)$$

Eq. (6) constitutes the linear system which is actually solved to find the displacement and pore pressure fields in time domain. The non-symmetric matrix arising from coupled poroelastic models takes on the following expression:

$$A = \left[ \theta K_1 + \frac{1}{\Delta t} K_2 \right] = \begin{bmatrix} \theta K & -\theta Q \\ \frac{Q^T}{\Delta t} & \theta H + \frac{P}{\Delta t} \end{bmatrix} \quad (7)$$

which may become ill-conditioned for small values of the time step  $\Delta t$  as will be shown in Section 3.

### 3. Definition of a critical time step $\Delta t_{crit}$

Let us consider a classical linear system  $A\mathbf{x} = \mathbf{b}$  where the matrix  $A$  is defined by Eq. (7). As was previously observed, in realistic simulations the number of nodal unknowns may be very large and the use of

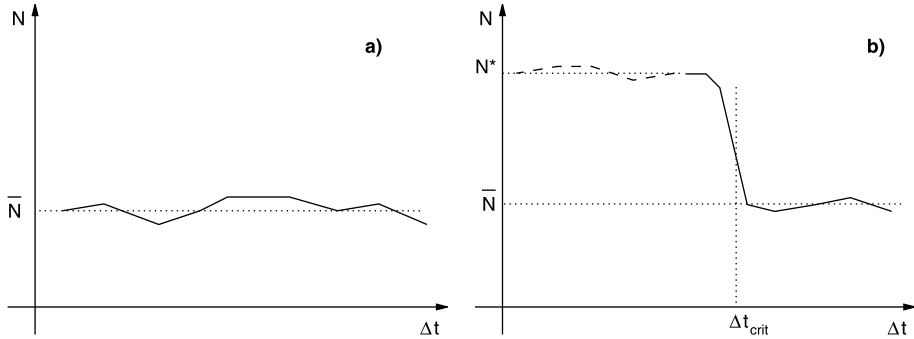


Fig. 1. Typical behavior of the number of iterations  $N$  when the time step  $\Delta t$  is decreased in a consolidation problem: (a) no ill-conditioning; (b) ill-conditioning occurs for  $\Delta t \leq \Delta t_{\text{crit}}$ .

an efficient projection solver appears to be quite appropriate. In the present paper we elect to use the algorithm Bi-CGSTAB (van ver Vorst, 1992) effectively preconditioned with the incomplete factorization with zero fill-in ILU(0) (Kershaw, 1978). We study the behavior of Bi-CGSTAB vs.  $\Delta t$  and expect the number of iterations  $N$  for convergence to increase significantly when  $\Delta t = \Delta t_{\text{crit}}$ .

Convergence is controlled by the relative norm of residual vector set to  $10^{-12}$  in the experiments that follow. When  $\Delta t$  is changed,  $N$  behaves in the two typical ways graphically depicted in Fig. 1. Inspection of this figure suggests that the matrices arising from coupled poroelastic models may be divided into two classes:

- type a:  $N$  is approximately stable around an average value  $\bar{N}$  for any  $\Delta t$  however small (Fig. 1a);
- type b:  $N$  is stable for  $\Delta t > \Delta t_{\text{crit}}$ . When  $\Delta t = \Delta t_{\text{crit}}$   $N$  suddenly increases to a new larger value  $N^*$ . For  $\Delta t < \Delta t_{\text{crit}}$ , Bi-CGSTAB may either still converge in  $N \simeq N^*$  iterations or break down (Fig. 1b).

If the matrix  $A$  exhibits a “type a” behavior, then we may argue that it is well-conditioned for any time step and that a lower bound for  $\Delta t$  does not exist. By contrast, if the matrix  $A$  exhibits a “type b” behavior, then ill-conditioning occurs at small time steps. In particular,  $\Delta t_{\text{crit}}$  is defined as the largest  $\Delta t$  for which the number of iterations increases to  $N^*$  much larger than  $\bar{N}$ .

### 3.1. Theoretical estimate of $\Delta t_{\text{crit}}$

In an ill-conditioned system two or more rows are nearly parallel. For example, the  $2 \times 2$  matrix:

$$A' = \begin{bmatrix} a_{11} & a_{12} \\ a_{21} & a_{22} \end{bmatrix}$$

is ill-conditioned if we have:

$$\frac{a_{11}}{a_{21}} \simeq \frac{a_{12}}{a_{22}}. \quad (8)$$

Let us try to extend the above condition to the poroelastic matrix (7). Applying Eq. (8) to the elements of the four blocks forming matrix  $A$  (see Eq. (7)), ill-conditioning is likely to occur if the coefficients of rows  $i$  and  $m$  satisfy the equation:

$$\frac{\theta K_{ij}}{\frac{\varrho_{m_i}^T}{\Delta t}} \simeq \frac{-\theta Q_{ik}}{\theta H_{mk} + \frac{P_{mk}}{\Delta t}} \quad j = 1, \dots, n_u \quad k = 1, \dots, n_p, \quad (9)$$

where  $n_u$  and  $n_p$  are the number of unknowns for nodal displacement and pore pressure, respectively. Eq. (9) can be interpreted as a condition depending upon  $\Delta t$ . The critical time step  $\Delta t_{\text{crit}}$  is by definition the  $\Delta t$  which satisfies Eq. (9).

The discussion about the existence of  $\Delta t_{\text{crit}}$  may be developed as follows. Write Eq. (9) as:

$$\Delta t \frac{\partial K_{ij}}{\partial Q_{mj}^T} \simeq \frac{-\Delta t \theta Q_{ik}}{\Delta t \theta H_{mk} + P_{mk}} \Rightarrow R_l(\Delta t) \simeq R_r(\Delta t)$$

and regard the above equation as a function of  $\Delta t$  only. It is observed that  $R_l(\Delta t)$  is a linearly increasing function of  $\Delta t$  while  $R_r(\Delta t)$  is a hyperbolic function with a horizontal asymptote for  $\Delta t \rightarrow \infty$  (Fig. 2). An intersection between  $R_l$  and  $R_r$  exists only if (Fig. 2):

$$\left[ \frac{dR_l}{d\Delta t} \right]_{\Delta t=0^+} < \left[ \frac{dR_r}{d\Delta t} \right]_{\Delta t=0^+}. \quad (10)$$

Eq. (10) can be easily converted to

$$\frac{\theta K_{ij}}{Q_{mj}^T} < \frac{-\theta Q_{ik}}{P_{mk}} \quad (11)$$

which represents a somewhat necessary condition for the existence of  $\Delta t_{\text{crit}}$ .

We now try to roughly estimate the magnitude of the terms belonging to the blocks which form the global matrix  $A$ . Ignoring the influence of the element geometry, the  $K$  coefficients are proportional to those of the elastic stress strain matrix  $D$  (see Appendix A), and hence have the same order of magnitude as the Young modulus  $E$ . For the sake of simplicity, we assume a value for the Poisson ratio  $\nu = 0.30$  so that  $E$  is the only representative mechanical parameter. Similarly, the  $H$  coefficients are approximately proportional to  $k/\gamma$  while the  $P$  coefficients can be represented by  $\Delta n \beta$ , where  $\Delta$  is a characteristic dimension of the finite element grid. In three-dimensional (3-D) problems,  $\Delta$  may be interpreted as the element volume, while in two-dimensional (2-D) or 3-D axisymmetric problems  $\Delta$  is an estimate of the element area. As an example, we focus on an axisymmetric porous medium discretized into elements with triangular cross-section, so  $\Delta$  can be regarded as the triangle area. The  $Q$  terms in axisymmetric problems can be locally viewed as the

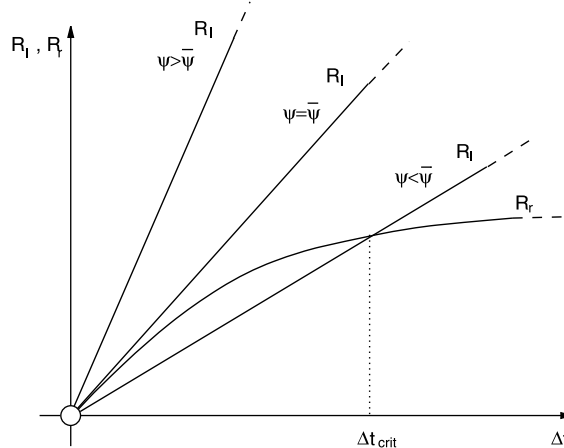


Fig. 2. Qualitative behavior of left-hand side  $R_l$  and right-hand side  $R_r$  of Eq. (9) vs.  $\Delta t$  and  $\psi = n\beta E$ .

projection of the triangle boundary over the coordinate directions (Gambolati et al., 2000a), and so they can be approximated by  $\sqrt{A}$ . Similar rough estimates for the coefficients of each single block have been recently used by other authors as well (Sloan and Abbo, 1999).

Substituting the above approximations into Eq. (9) and disregarding the minus sign on the right-hand side leads to:

$$\frac{\theta E}{\frac{\sqrt{A}}{\Delta t}} \simeq \frac{\theta \sqrt{A}}{\theta \frac{k}{\gamma} + \frac{4n\beta}{\Delta t}}$$

from which, looking for an explicit expression of  $\Delta t$ , we obtain:

$$\Delta t = \Delta t_{\text{crit}} \simeq \left( \frac{1 - n\beta E}{\theta} \right) \frac{4\gamma}{kE}. \quad (12)$$

It can be easily verified that the right-hand side of Eq. (12) has the unit of a time, as was expected, with  $((1 - n\beta E)/\theta)$  a dimensionless factor.

By the way in which it has been derived, Eq. (12) represents a very crude estimate of the critical time step. Nevertheless, Eq. (12) may prove able to capture the basic relation between  $\Delta t_{\text{crit}}$  and the physical parameters of the porous medium ( $E$ ,  $k$ ,  $n$  and  $\beta$ ) through a characteristic measure of the triangulation ( $A$ ). More generally, we can write  $\Delta t_{\text{crit}}$  as:

$$\Delta t_{\text{crit}} = \chi(\psi, \theta) \frac{4\gamma}{kE} \quad (13)$$

with  $\psi = n\beta E$  and  $\chi$  an unknown dimensionless factor depending upon  $\psi$ ,  $\theta$  and the shape and resolution of the mesh. So Eq. (13) may be viewed only as a qualitative equation which cannot be practically used to assess the accurate critical time step but can supply interesting information on the factors which affect  $\Delta t_{\text{crit}}$ .

From Eq. (11) we can derive a necessary condition for the existence of  $\Delta t_{\text{crit}}$ . If we replace in Eq. (11) the aforementioned approximations for the coefficients we obtain:

$$\frac{E}{\sqrt{A}} < \bar{\psi} \frac{\sqrt{A}}{4n\beta}, \quad (14)$$

where  $\bar{\psi}$  is an unknown factor which accounts for the quantities we have neglected in our crude estimate. Basically,  $\bar{\psi}$  depends upon the shape of the triangles and to a lesser extent on the Poisson ratio. From Eq. (14) we get:

$$n\beta E < \bar{\psi} \Rightarrow \psi < \bar{\psi}. \quad (15)$$

A graphical interpretation of the implication Eq. (15) is given in Fig. 2.

Thus, it can be argued that a  $\bar{\psi}$  value exists for  $\psi$  above which the matrix  $A$  will always be well conditioned and will show the “type a” behavior of Fig. 1. By distinction, when  $\psi < \bar{\psi}$  matrix  $A$  will show the “type b” behavior with a critical time step that, according to Eq. (13), is expected to increase for coarser grids and less permeable and softer porous media. However, deviations from this conceptual scheme are possible in difficult problems depending on the actual behavior of the unknown function  $\chi$ .

### 3.2. Subcritical and super-critical $\Delta t$

Eq. (13) defines the critical time step yielding ill-conditioning but does not explicitly give an indication as to the matrix conditioning when  $\Delta t \neq \Delta t_{\text{crit}}$ , i.e. when  $\Delta t > \Delta t_{\text{crit}}$  (super-critical time step) or  $\Delta t < \Delta t_{\text{crit}}$  (subcritical time step).

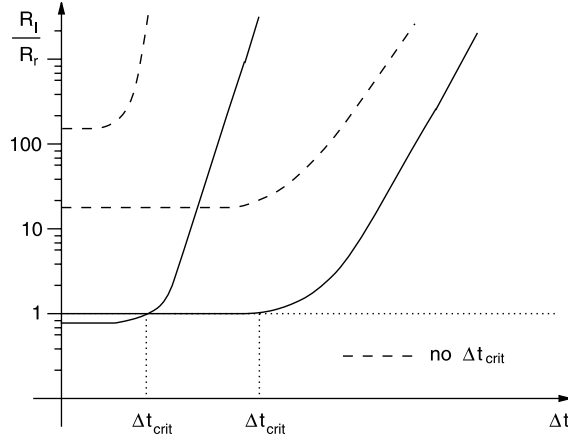


Fig. 3. Qualitative behavior of the ratio  $R_l/R_r$  vs. the time step  $\Delta t$ .

The problem conditioning depends primarily on the ratio  $R_l/R_r$ . As can be seen from Fig. 2, for  $\Delta t > \Delta t_{\text{crit}}$   $R_l/R_r$  grows with the time step size, so the matrix parallelism reduces and the system is consequently well conditioned. By distinction, for  $\Delta t < \Delta t_{\text{crit}}$   $R_l/R_r$  may remain close to 1 for any  $\Delta t$  and conditioning can still be critical, as is illustrated in Fig. 1b and will be shown later with practical examples.

Another interesting remark can be derived from the analysis of Fig. 3 which graphically represents the behavior of  $R_l/R_r$  vs.  $\Delta t$ . Irrespective of the existence of  $\Delta t_{\text{crit}}$ , Eq. (9) shows that  $R_l/R_r$  stabilizes when  $\Delta t$  goes to zero as the directions of the matrix rows are practically preserved, hence conditioning does not change. When  $R_l/R_r \approx 1$  (solid profiles of Fig. 3) the critical condition has been achieved and the numerical problem becomes ill-conditioned with possible ill-conditioning for any  $\Delta t < \Delta t_{\text{crit}}$ . When  $R_l/R_r$  is always larger than 1 (dashed profiles of Fig. 3)  $\Delta t_{\text{crit}}$  does not exist and conditioning is good for any  $\Delta t$  value.

### 3.3. Comparison with critical time steps by other authors

In the previous sections, we have discussed a critical time step  $\Delta t_{\text{crit}}$  below which the numerical solution to the FE consolidation model may become difficult because of ill-conditioning. A different lower limit for  $\Delta t$  was derived by Vermeer and Verruijt (1981) by prescribing a condition to limit the development of numerical oscillations of the pore pressure solution in a porous column subject to an instantaneous load. This bound was explicitly calculated for one-dimensional (1-D) consolidation as:

$$\Delta t \geq \frac{1}{6} \frac{(\Delta h)^2}{\theta c},$$

where  $c$  is the so-called consolidation coefficient and  $\Delta h$  a characteristic size of the FE grid. Consistent with the notation used in the present paper, we can write:

$$c = \frac{k}{\gamma(c_M + n\beta)} \quad (\Delta h)^2 \simeq A$$

with  $c_M$  the vertical soil compressibility. As is well known:

$$c_M = \frac{(1+v)(1-2v)}{1-v} \frac{1}{E} \simeq \frac{1}{E}$$

and the lower  $\Delta t$  bound according to Vermeer and Verruijt (1981) is:

$$\Delta t \geq \frac{1}{6} \frac{\Delta}{\theta} \frac{\gamma(1+n\beta E)}{kE} = \left( \frac{1+\psi}{6\theta} \right) \frac{\Delta\gamma}{kE},$$

that is

$$\Delta t_{\text{crit}} = \chi'(\psi, \theta) \frac{\Delta\gamma}{kE}. \quad (16)$$

This outcome is obtained for 1-D problems but the authors argue that a similar expression holds true for 2-D and 3-D problems as well.

It is interesting to observe that, although the critical time step has a different implication in the two derivations, Eq. (16) of Vermeer and Verruijt (1981) is surprisingly similar to our Eq. (13). The main difference consists of the behavior of the weighting factor  $\chi'$  vs.  $\psi$ . In fact, while in our case a  $\psi$  value may be found above which there is no  $\Delta t_{\text{crit}}$  yielding ill-conditioning, Vermeer and Verruijt (1981)  $\chi'$  can never be zero or negative, and hence a lower bound for the solution stability always exists in their derivation.

Another interesting remark can be made for the case of an incompressible fluid ( $\beta = 0$ ). Even though this assumption can be disputed on physical grounds (Chierici, 1989), it has been used by a number of authors in coupled poroelastic problems (Ghaboussi and Wilson, 1973; Reed, 1984; Lewis and Schrefler, 1987; Sloan and Abbo, 1999) and is quite acceptable in shallow compressible rocks. According to the present development, if  $\beta = 0$  then  $\psi = 0 < \bar{\psi}$  (see Eq. (15)) and so  $\chi = \chi_0 > 0$ . Thus the critical time step turns to be:

$$\Delta t_{\text{crit}} = \chi_0 \frac{\Delta\gamma}{kE} \quad (17)$$

and it does exist for any poroelastic problem. This conclusion was first remarked by Ghaboussi and Wilson (1973) who also suggested a criterion for the choice of a minimum  $\Delta t$  value. The criterion of Ghaboussi and Wilson (1973) is based on the assumption that the greatest difficulties are met in stiff and low permeable porous media. However, the present analysis provides evidence that the critical time step is not related to  $E/k$  but rather to  $1/(kE)$ . This implies that if, for example,  $E = 10^4$  kg/m<sup>2</sup> and  $k = 10^{-4}$  m/s (compressible and permeable soil) conditioning is worse than with  $E = 10^8$  kg/m<sup>2</sup> and  $k = 10^{-7}$  m/s (stiff and low permeable soil).

The numerical examples discussed below show clearly that stiff porous systems are generally better conditioned than soft media, irrespective of permeability, i.e. quite different from the outcome of Ghaboussi and Wilson (1973).

#### 4. Numerical results

A number of numerical experiments have been performed to substantiate the above theoretical arguments. An axisymmetric poroelastic problem is considered with a unit pore pressure decline prescribed at the middle node of the symmetry axis. The  $1000 \times 2000$  m domain of Fig. 4 is variably discretized into triangular elements. Standard Dirichlet conditions with zero displacement and pore pressure change on the outer and bottom boundaries, zero radial displacement on the symmetry axis, and zero pore pressure decline on the top boundary are prescribed (Fig. 4). The porous medium is assumed to be fully saturated by groundwater ( $\gamma = 1000$  kg/m<sup>3</sup>,  $\beta = 4 \times 10^{-5}$  cm<sup>2</sup>/kg) with a uniform porosity  $n = 0.28$  and Poisson ratio  $\nu = 0.30$ . Finally, an Euler backward marching scheme is adopted ( $\theta = 1$ ).

According to Eq. (13) and with the previous assumptions the critical time step basically depends upon the three parameters  $E$ ,  $k$  and  $\Delta$ . The numerical experiments can thus concern three problems:

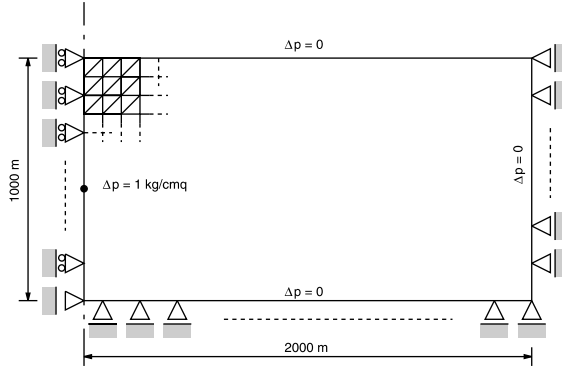


Fig. 4. Cross-section of the axisymmetric poroelastic sample problem with the indication of geometry, boundary conditions and (regular) triangulation.

- *problem 1*:  $k$  varies with  $E$  and  $\Delta$  constant (constant  $\psi$ );
- *problem 2*:  $\Delta$  varies with  $E$  and  $k$  constant (constant  $\psi$ );
- *problem 3*:  $E$  varies with  $k$  and  $\Delta$  constant (variable  $\psi$ ).

Furthermore, problems 1 and 2 are split into two parts (problems 1a, 1b and 2a, 2b) accounting for two different values of  $E$ , yielding (a)  $\psi$  smaller and (b)  $\psi$  larger than  $\bar{\psi}$ .

The matrix conditioning in each numerical experiment is measured by the use of the following indexes (Westlake, 1968):

$$L = \frac{|\lambda_1|}{|\lambda_n|}, \quad (18)$$

$$D = \frac{\prod_{i=1}^n \left( \sum_{j=1}^n a_{ij}^2 \right)^{1/2}}{|\det A|}, \quad (19)$$

where  $\lambda_1$  and  $\lambda_n$  are the maximum and minimum eigenvalue of the matrix  $A$  and  $a_{ij}$  the  $A$  coefficients. Ill-conditioning of matrix  $A$  is indicated by large values of both  $L$  and  $D$ .

The behavior of  $L$  and  $D$  vs.  $\Delta t$  is studied and is related to the Bi-CGSTAB rate of convergence. Obviously, we expect  $L$  and  $D$  to increase significantly for  $\Delta t = \Delta t_{\text{crit}}$ , and correspondingly Bi-CGSTAB to converge much more slowly or even to fail.

#### 4.1. Problem 1a: changing $k$ with $\psi < \bar{\psi}$

We assume a homogeneous porous medium with a stiffness such that  $\psi = 0.022$ , which corresponds to  $E = 2 \times 10^3 \text{ kg/cm}^2$ , a typical value of the sediments of the upper Po river basin, Italy (Gambolati et al., 2000b). A regular triangulation is used with  $\Delta r = \Delta z = 25 \text{ m}$ , and  $\Delta = 312.5 \text{ m}^2$ .

Fig. 5 gives the number of iterations  $N$  and index  $L$  vs.  $\Delta t$ . The critical time step is easily identified with both  $N$  and  $L$  growing when the problem becomes ill-conditioned. The value of the unknown factor  $\chi$  (Eq. (13)), depending upon  $\psi$  (i.e. ultimately on  $E$ ),  $\theta$  and the shape and resolution of the grid, can be back calculated from the experimental  $\Delta t_{\text{crit}}$  found in the first simulation with  $k = 10^{-4} \text{ m/s}$ , thus obtaining  $\chi = 6.4 \times 10^{-3}$ . By the use of this value the theoretical  $\Delta t_{\text{crit}}$  for the other two problems is computed and compared in Table 1 with the experimental  $\Delta t_{\text{crit}}$ , pointing out an excellent agreement.

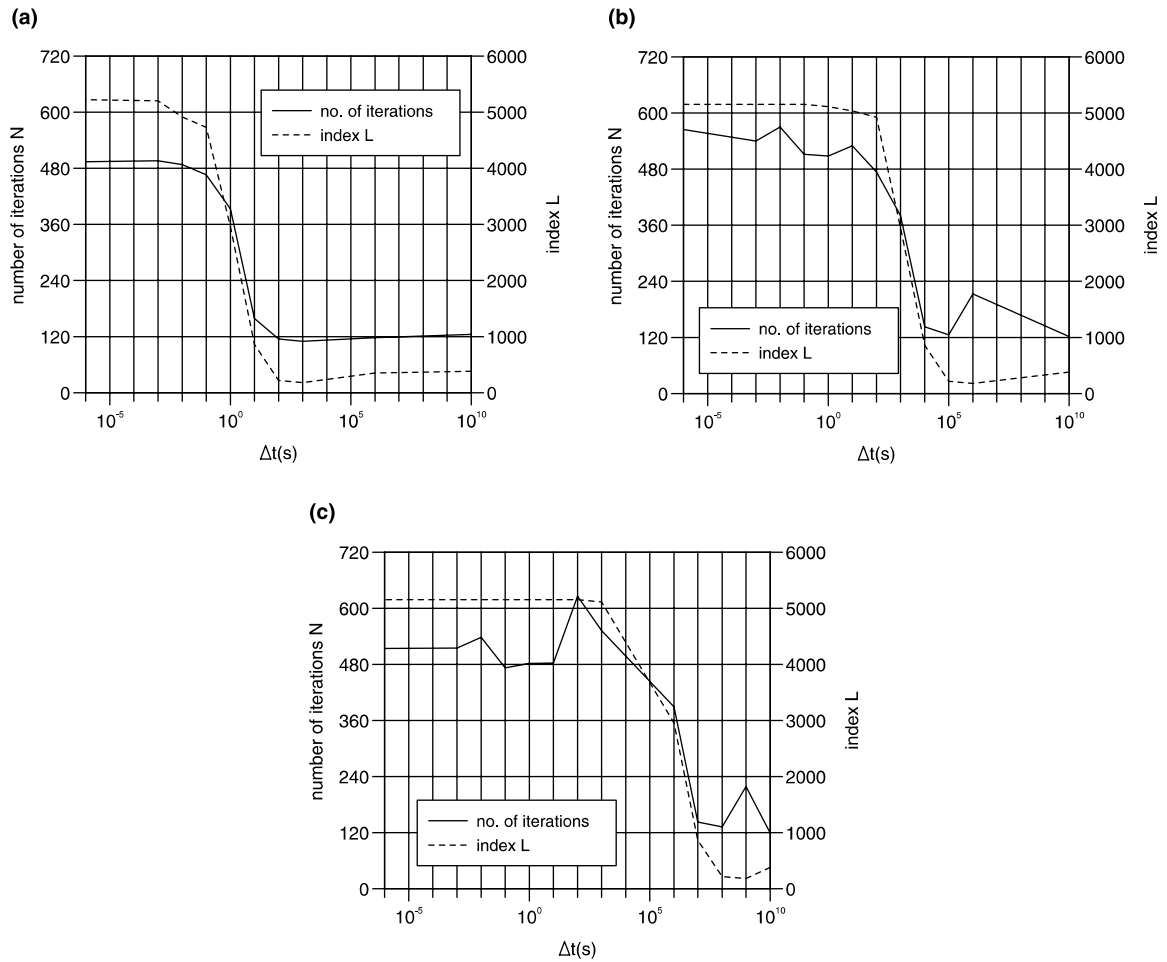


Fig. 5. Problem 1a: number of iterations  $N$  and index  $L$  vs.  $\Delta t$  for  $\psi = 0.022$ ,  $A = 312.5 \text{ m}^2$  and (a)  $k = 10^{-4} \text{ m/s}$ ; (b)  $k = 10^{-7} \text{ m/s}$ ; (c)  $k = 10^{-10} \text{ m/s}$ .

Table 1

Problem 1a: experimental and theoretical  $\Delta t_{\text{crit}}$  vs.  $k$  with  $\psi = 0.022$  and  $A = 312.5 \text{ m}^2$  using  $\chi = 6.4 \times 10^{-3}$  back calculated from the problem with  $k = 10^{-4} \text{ m/s}$

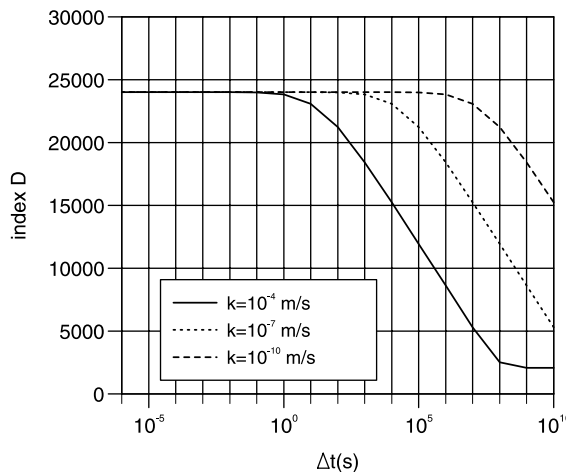
$k$ (m/s)	Theoretical $\Delta t_{\text{crit}}$ (s)	Experimental $\Delta t_{\text{crit}}$ (s)	$\bar{N}$	$N^*$
$10^{-4}$	—	1	110	490
$10^{-7}$	$10^3$	$10^3$	130	550
$10^{-10}$	$10^6$	$10^6$	130	520

Table 2 provides  $|\lambda_1|$ ,  $|\lambda_n|$  and  $L$  for the sample problem with  $k = 10^{-4} \text{ m/s}$ . It is interesting to observe that the  $L$  increase is due to an increase of  $|\lambda_1|$  while  $|\lambda_n|$  remains practically stable. Index  $D$  is shown in Fig. 6. As expected  $D$  achieves its maximum value for  $\Delta t = \Delta t_{\text{crit}}$  thus providing evidence that some matrix rows are nearly parallel (when they are exactly parallel  $\det A = 0$ ).

Table 2

Problem 1a: maximum and minimum eigenvalue of  $A$  for  $\psi = 0.022$ ,  $\Delta = 312.5 \text{ m}^2$  and  $k = 10^{-4} \text{ m/s}$ 

$\Delta t$ (s)	$ \lambda_1 $	$ \lambda_n $	$L$
$10^{10}$	1.03	$0.26 \times 10^{-2}$	396
$10^6$	1.37	$0.39 \times 10^{-2}$	351
$10^3$	1.38	$0.75 \times 10^{-2}$	184
$10^2$	1.51	$0.69 \times 10^{-2}$	219
$10^1$	3.97	$0.46 \times 10^{-2}$	863
$10^0$	8.87	$0.30 \times 10^{-2}$	2957
$10^{-1}$	12.3	$0.26 \times 10^{-2}$	4731
$10^{-2}$	12.8	$0.26 \times 10^{-2}$	4915
$10^{-3}$	13.5	$0.26 \times 10^{-2}$	5204
$10^{-6}$	13.6	$0.26 \times 10^{-2}$	5223

Fig. 6. Problem 1a: index  $D$  vs.  $\Delta t$  for  $\psi = 0.022$ ,  $\Delta = 312.5 \text{ m}^2$  and different  $k$  values.

A non-homogeneous case has also been addressed for a stratified porous medium with alternating sand and clay layers ( $k = 10^{-4}$  and  $10^{-7} \text{ m/s}$ , respectively). The  $N$  and  $L$  values are supplied in Fig. 7. Note that ill-conditioning is found for  $\Delta t_{\text{crit}} = 1 \text{ s}$  (the same  $\Delta t_{\text{crit}}$  as for the homogeneous case with  $k = 10^{-4} \text{ m/s}$ ) with some probable ill-conditioning also for a very large  $\Delta t$ . Table 3 gives the maximum and minimum eigenvalues for the non-homogeneous problem. Inspection of Table 3 suggests that ill-conditioning occurring at  $\Delta t = \Delta t_{\text{crit}}$  is due to an increase of  $|\lambda_1|$  as in Table 2 while ill-conditioning at the largest  $\Delta t$  is related to a decrease of  $|\lambda_n|$ .

#### 4.2. Problem 1b: changing $k$ with $\psi > \bar{\psi}$

In this section the same simulations as in Section 4.1 are performed, except for  $E$  which is increased by one order of magnitude ( $E = 2 \times 10^4 \text{ kg/cm}^2$ ) with  $\psi = 0.22$ . The experimental results are reported in Fig. 8 and Table 4. In these examples matrix  $A$  exhibits the “type a” behavior of Fig. 1. This choice of  $E$  produces  $\psi > \bar{\psi}$  and so, as is theoretically expected, there is no  $\Delta t_{\text{crit}}$  and  $A$  is well conditioned for any time step size.

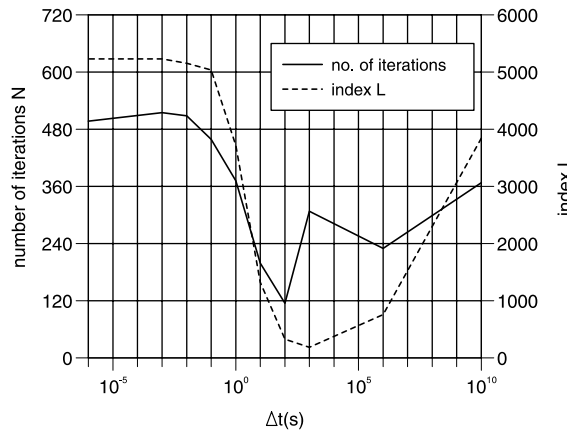


Fig. 7. Number of iterations  $N$  and index  $L$  vs.  $\Delta t$  for the non-homogeneous problem with  $\psi = 0.022$ ,  $\Delta = 312.5 \text{ m}^2$  and  $k$  equal to  $10^{-7} \text{ m/s}$  (clay) and  $10^{-4} \text{ m/s}$  (sand).

Table 3

Non-homogeneous sample problem: maximum and minimum eigenvalue of  $A$  for  $\psi = 0.022$ ,  $\Delta = 312.5 \text{ m}^2$  and  $k$  equal to  $10^{-7} \text{ m/s}$  (clay) and  $10^{-4} \text{ m/s}$  (sand)

$\Delta t$ (s)	$ \lambda_1 $	$ \lambda_n $	$L$
$10^{10}$	1.03	$0.26 \times 10^{-3}$	3960
$10^6$	1.37	$0.18 \times 10^{-2}$	761
$10^3$	1.40	$0.74 \times 10^{-2}$	189
$10^2$	2.07	$0.71 \times 10^{-2}$	329
$10^1$	5.29	$0.40 \times 10^{-2}$	1323
$10^0$	10.4	$0.28 \times 10^{-2}$	3714
$10^{-1}$	13.1	$0.26 \times 10^{-2}$	5038
$10^{-2}$	13.4	$0.26 \times 10^{-2}$	5154
$10^{-3}$	13.6	$0.26 \times 10^{-2}$	5231
$10^{-6}$	13.6	$0.26 \times 10^{-2}$	5231

#### 4.3. Problem 2a: changing $\Delta$ with $\psi < \bar{\psi}$

We assume a homogeneous medium with  $E = 2 \times 10^3 \text{ kg/cm}^2$  ( $\psi = 0.022$ ) and  $k = 10^{-4} \text{ m/s}$  and analyze the influence of  $\Delta$  on conditioning by changing the radial spacing  $\Delta r$  or the vertical spacing  $\Delta z$  or both. The main results are summarized in Table 5. It may be observed that the way in which the  $\Delta$  variation is implemented has some influence on the matrix behavior. In particular, comparison of the second and third rows of Table 5, where  $\Delta_{\max}$  is approximately the same, shows that a variation of  $\Delta r$  is much more significant on  $\Delta t_{\text{crit}}$  magnitude than a variation of  $\Delta z$ . This is probably due to the fact that in axisymmetric problems the volume integration over the annular elements is more influenced by  $r$  rather than by  $z$  (Gambolati et al., 2000a). Nevertheless, we can note that, if  $\Delta$  varies because  $\Delta r$  varies (first and second rows of Table 5), then Eq. (13) still substantially holds as  $\Delta t_{\text{crit}}$  change is almost proportional to the variation of  $\Delta_{\max}$ . Also observe that  $\Delta t_{\text{crit}}$  of the fourth row is equal to that of the first row although  $\Delta_{\max}$  of the former is much larger than that of the latter since the smaller elements of a non-uniform mesh attenuate the effects of the larger ones.

Fig. 9 shows the results corresponding to  $\Delta r$  and  $\Delta z$  of the second row of Table 5 with the others very similar except for the problem with a uniform mesh which is the same as that of Fig. 5a. It might be

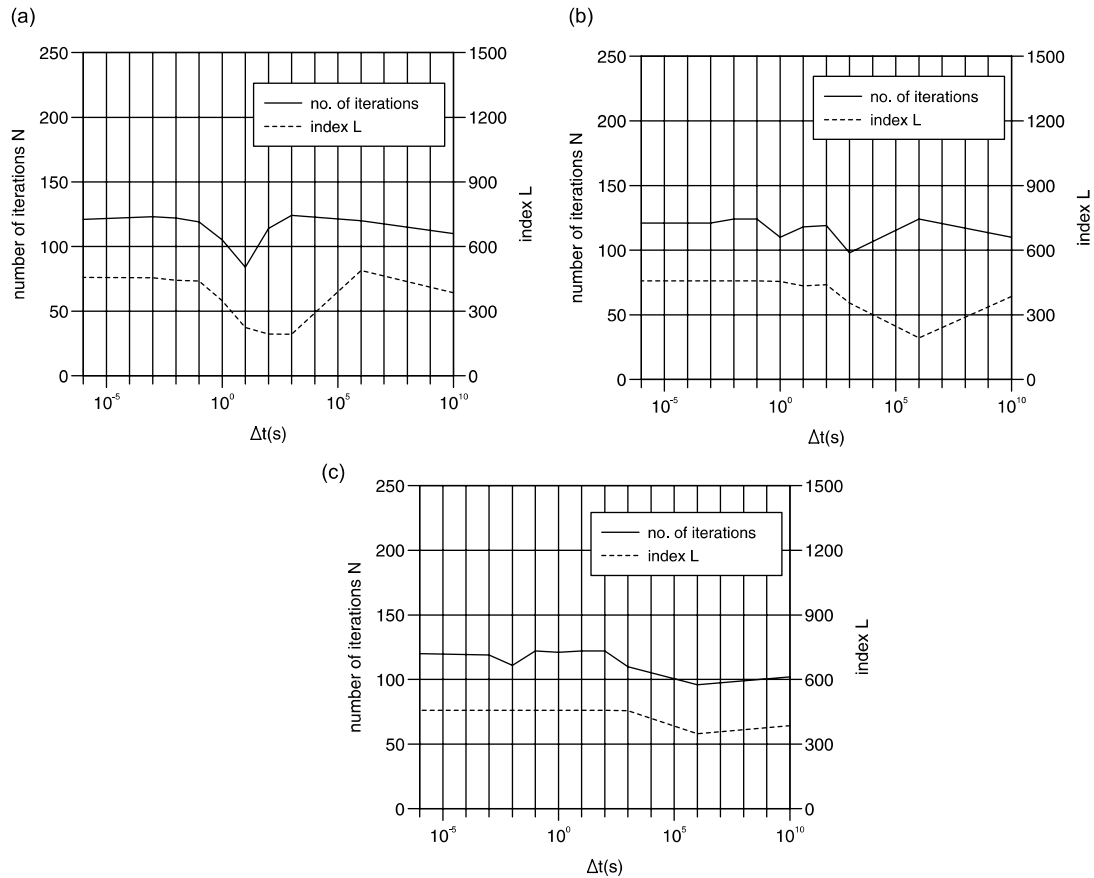


Fig. 8. Problem 1b: number of iterations  $N$  and index  $L$  vs.  $\Delta t$  for  $\psi = 0.22$ ,  $\Delta = 312.5 \text{ m}^2$  and: (a)  $k = 10^{-4} \text{ m/s}$ ; (b)  $k = 10^{-7} \text{ m/s}$ ; (c)  $k = 10^{-10} \text{ m/s}$ .

Table 4

Problem 1b: experimental  $\Delta t_{\text{crit}}$  vs.  $k$  with  $\psi = 0.22$  ( $\psi > \bar{\psi}$ ) and  $\Delta = 312.5 \text{ m}^2$

$k$ (m/s)	Experimental $\Delta t_{\text{crit}}$ (s)	$\bar{N}$	$N^*$
$10^{-4}$	—	100	—
$10^{-7}$	—	110	—
$10^{-10}$	—	120	—

Table 5

Problem 2a: experimental  $\Delta t_{\text{crit}}$  vs.  $\Delta_{\text{max}}$  with  $\psi = 0.022$  and  $k = 10^{-4} \text{ m/s}$

$\Delta r$ (m)	$\Delta z$ (m)	$\Delta_{\text{max}}$ ( $\text{m}^2$ )	Experimental $\Delta t_{\text{crit}}$ (s)	$\bar{N}$	$N^*$
25	25	312.5	1	110	490
2–396	10	1978.5	10	130	Failure
20	1–200	2000	1	110	Failure
1–189	0.5–200	18910	1	150	Failure

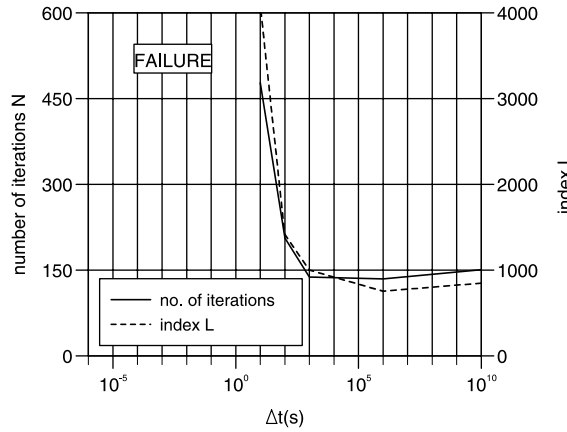


Fig. 9. Problem 2a: number of iterations  $N$  and index  $L$  vs.  $\Delta t$  for  $\psi = 0.022$ ,  $k = 10^{-4}$  m/s and  $A_{\max} = 1978.5$  m<sup>2</sup> (variable radial spacing  $\Delta r$ ).

observed that, for  $\Delta t \leq \Delta t_{\text{crit}}$ , the ill-conditioning is so severe that Bi-CGSTAB fails to converge (exhibiting either an incredibly slow convergence rate or a diverging residual) and the index  $L$  takes on a very large value.

#### 4.4. Problem 2b: changing $\Delta$ with $\psi > \bar{\psi}$

We address the same sample problems as in Section 4.3 with  $E = 2 \times 10^4$  kg/cm<sup>2</sup> and  $\psi = 0.22$ . Similarly to Section 4.2, we would expect  $\psi > \bar{\psi}$  with no critical time step.

The main results are summarized in Table 6. We can note that one example produces a  $\Delta t_{\text{crit}}$ . This should be no surprise since  $\bar{\psi}$  is sensitive to the element geometry, and so most probably the new discretization of this example is such that  $\psi$  does not exceed  $\bar{\psi}$ .

Fig. 10 shows the results corresponding to  $\Delta r$  and  $\Delta z$  of the second and third rows of Table 6 since the case with the uniform mesh is the same as in Fig. 8a and the remaining test case behaves similarly to Fig. 10b.

#### 4.5. Problem 3: changing $E$

In this final group of computational experiments we study the influence of a variation of  $E$ , and hence of  $\psi$ , within a mechanically heterogeneous porous medium. To simulate a realistic configuration, the compressibility profile vs.  $z$  of the sedimentary Po river basin, Italy (Gambolati et al., 2000b) is used and

Table 6

Problem 2b: experimental  $\Delta t_{\text{crit}}$  vs.  $\Delta t$  with  $\psi = 0.22$  and  $k = 10^{-4}$  m/s

$\Delta r$ (m)	$\Delta z$ (m)	$A_{\max}$ (m <sup>2</sup> )	Experimental $\Delta t_{\text{crit}}$ (s)	$\bar{N}$	$N^*$
25	25	312.5	–	100	–
2–396	10	1978.5	$10^{-1}$	200	Failure
20	1–200	2000	–	150	–
1–189	0.5–200	18910	–	110	–

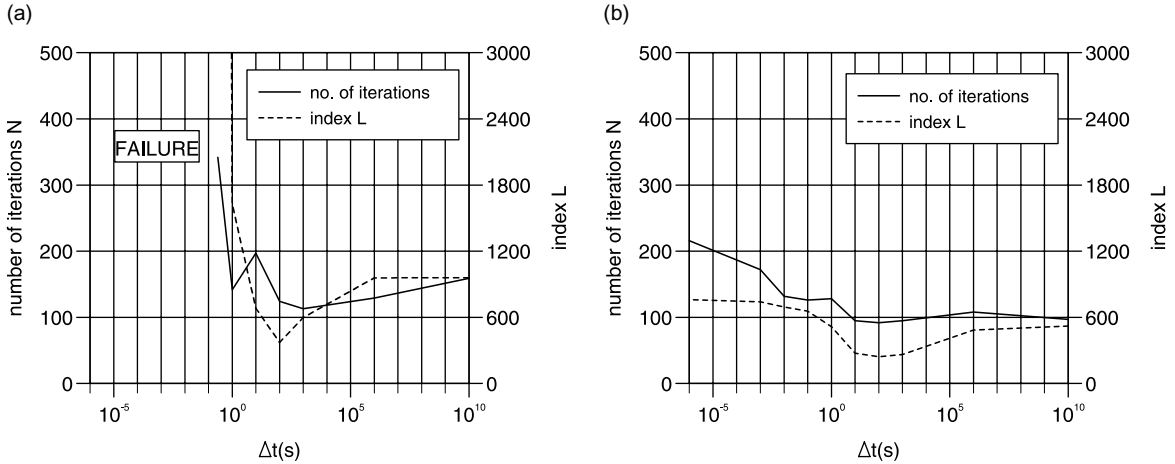


Fig. 10. Problem 2b: number of iterations  $N$  and index  $L$  vs.  $\Delta t$  for  $\psi = 0.22$ ,  $k = 10^{-4}$  m/s and (a)  $\Delta_{\max} = 1978.5$  m $^2$  (variable radial spacing  $\Delta r$ ) and (b)  $\Delta_{\max} = 2000$  m $^2$  (variable vertical spacing  $\Delta z$ ).

different examples are generated by properly scaling this profile. We assume  $k = 10^{-4}$  m/s throughout and a uniform mesh with  $\Delta r = \Delta z = 25$  m and  $\Delta = 312.5$  m $^2$ .

The behavior of  $N$ ,  $L$  and  $D$  vs.  $\Delta t$  is supplied in Figs. 11 and 12 where  $\Delta t_{\text{crit}}$  may be easily found.

Table 7 summarizes the most significant results and provides as a reference  $E$  value the smallest (i.e. the shallowest) one. The overall  $E$  variation with  $z$  is about two orders of magnitude. Careful inspection of Table 7 reveals that Eq. (13) substantially holds true, and there is no critical time step as long as the stiffness is adequately increased such that  $\psi > \bar{\psi}$ . It should be noted that the global effect of the mechanical heterogeneity is that of offsetting the influence of the smaller Young moduli.

## 5. Suggestions for remediating ill-conditioning

Ill-conditioning of FE poroelastic equations can be so severe that a projection solver may fail to converge, as is indicated by a few sample problems discussed in the previous section. In these examples the common scaling algorithm as is usually implemented (i.e. scaling by the diagonal term) appears to be quite ineffective. In fact, while it may yield a little acceleration of convergence when the solver works, it gives no benefit when it breaks down.

The present analysis may suggest that ill-conditioning can be avoided by changing the mesh resolution so as to produce a  $\Delta t_{\text{crit}}$  (see Eq. (13)) smaller than the minimum  $\Delta t$  required by the simulation. A practical way to estimate a priori  $\Delta t_{\text{crit}}$  in a coupled poroelastic problem is to analyze the behavior of the ill-conditioning index  $D$  vs.  $\Delta t$ , which is quite inexpensive. As can be seen from Figs. 6 and 12,  $\Delta t_{\text{crit}}$  is roughly denoted by the beginning of the leftmost flat portion of the curve.

Finally, a way to solve severely ill-conditioned problems might be improving the quality of the preconditioner. For example, the incomplete LU factorization with threshold strategies (ILUT) preconditioner (Saad, 1994), although usually more expensive than other preconditioners such as ILU(0), which is used in the present analysis, may sometimes succeed in converging when ILU(0) leads to failure. As an example, a comparison between the convergence profiles of Bi-CGSTAB preconditioned with ILU(0) and ILUT, using optimal fill-in level and tolerance parameters (see for instance Saad (1996)), is shown in Fig. 13 for two test cases discussed in Section 4. Note that preconditioner ILUT allows for a significant acceleration of

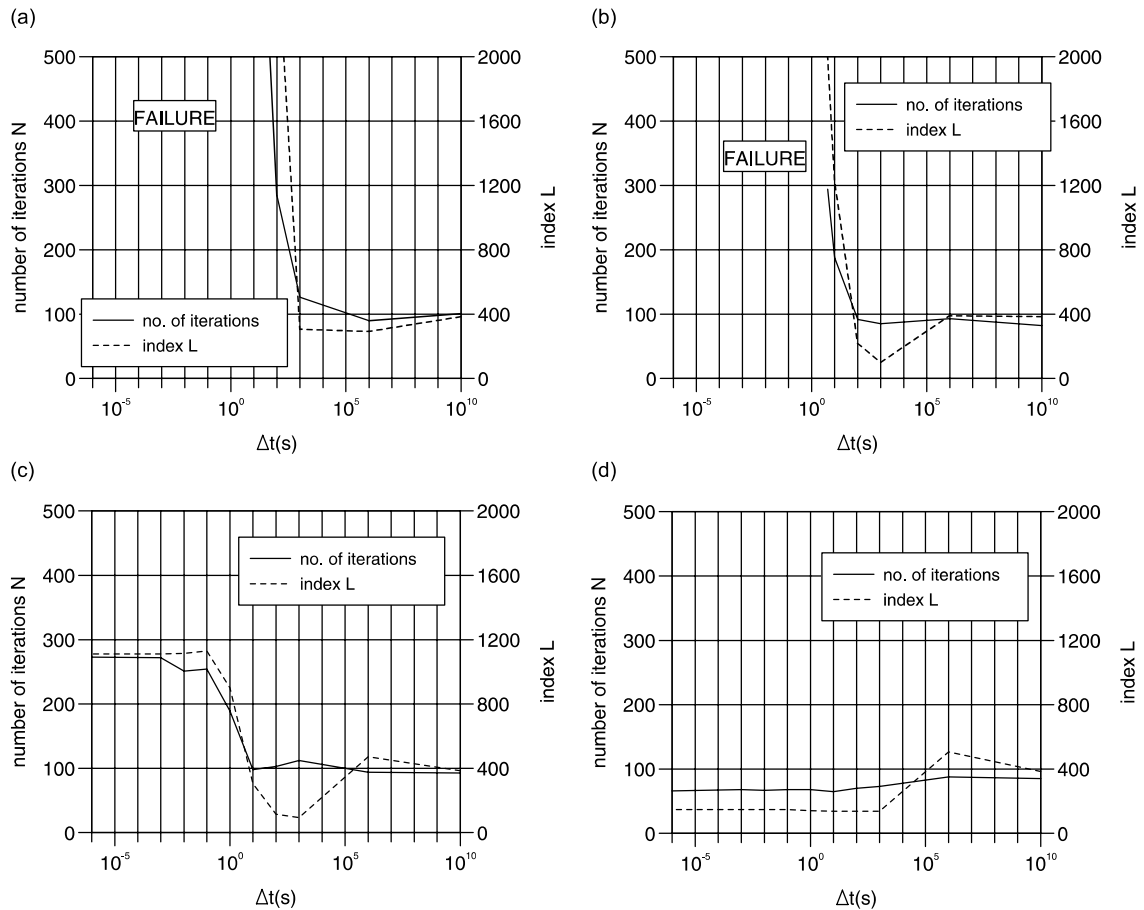


Fig. 11. Problem 3: number of iterations  $N$  and index  $L$  vs.  $\Delta t$  for  $k = 10^{-4}$  m/s,  $\Delta = 312.5$  m $^2$  and (a)  $\psi_{\min} = 8 \times 10^{-5}$ , (b)  $\psi_{\min} = 8 \times 10^{-4}$ , (c)  $\psi_{\min} = 8 \times 10^{-3}$ , (d)  $\psi_{\min} = 8 \times 10^{-1}$ .

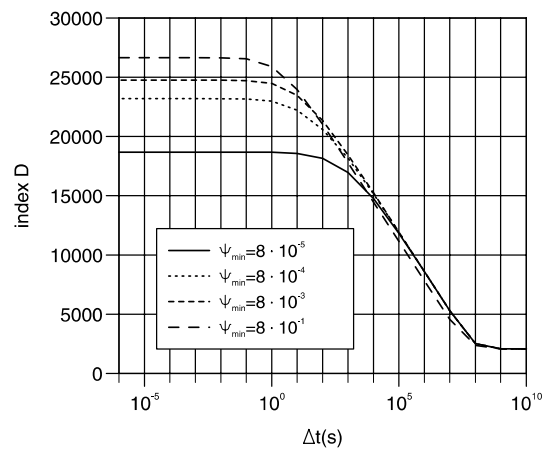


Fig. 12. Problem 3:  $D$  vs.  $\Delta t$  for  $k = 10^{-4}$  m/s,  $\Delta = 312.5$  m $^2$  and different  $\psi_{\min}$ .

Table 7

Problem 3: experimental  $\Delta t_{\text{crit}}$  vs.  $E$  for a compressibility profile similar to that of the Po river basin with  $k = 10^{-4}$  m/s and  $\Delta = 312.5$  m<sup>2</sup>. The smallest (i.e. shallowest)  $E$  value is given

$E_{\text{min}}$ (kg/m <sup>2</sup> )	$\psi_{\text{min}}$	Experimental $\Delta t_{\text{crit}}$ (s)	$\bar{N}$	$N^*$
$6 \times 10^4$	$8 \times 10^{-5}$	10	130	Failure
$6 \times 10^5$	$8 \times 10^{-4}$	1	90	Failure
$6 \times 10^6$	$8 \times 10^{-3}$	$10^{-1}$	90	270
$6 \times 10^8$	$8 \times 10^{-1}$	—	65	—

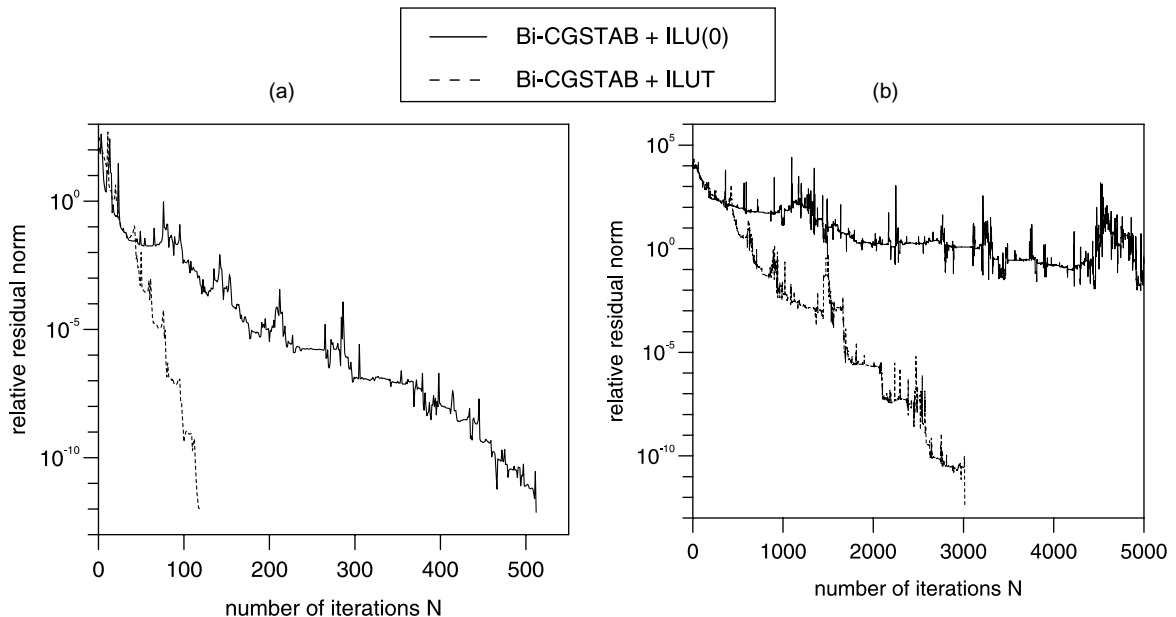


Fig. 13. Comparison between the convergence profiles of Bi-CGSTAB preconditioned with ILU(0) and ILUT for the problems: (a) regular mesh ( $\Delta r = \Delta z = 25$  m,  $\Delta = 312.5$  m<sup>2</sup>),  $k = 10^{-7}$  m/s and  $E = 2 \times 10^7$  kg/m<sup>2</sup> with  $\Delta t = 10^{-1}$  s ( $\Delta t < \Delta t_{\text{crit}} = 10^3$  s); and (b) regular mesh ( $\Delta r = \Delta z = 25$  m,  $\Delta = 312.5$  m<sup>2</sup>),  $k = 10^{-4}$  m/s and  $E_{\text{min}} = 6 \times 10^4$  kg/m<sup>2</sup> with  $\Delta t = 1$  s ( $\Delta t < \Delta t_{\text{crit}} = 10$  s).

convergence in a difficult problem (Fig. 13a) and for convergence in a problem where ILU(0) practically fails (Fig. 13b).

## 6. Conclusions

In the FE solution of coupled poroelasticity problems difficulties can be encountered for small time integration steps  $\Delta t$  because the global matrix  $A$  may be ill-conditioned. For a given problem and a given grid conditioning of  $A$  depends on  $\Delta t$ . A critical value  $\Delta t_{\text{crit}}$  may exist for which ill-conditioning occurs and persists also for  $\Delta t < \Delta t_{\text{crit}}$ . Under such circumstances the FE equations may be difficult to solve with preconditioned conjugate gradient like solvers, such as Bi-CGSTAB, experiencing a slow convergence or even failure. An empirical expression for  $\Delta t_{\text{crit}}$  is derived showing that:

- $\Delta t_{\text{crit}}$  is larger when coarser finite element meshes are used;
- in axisymmetric problems, conditioning of  $A$  is especially sensitive to the variation of the radial spacing;
- contrary to what one might expect stiff low permeable porous systems are not necessarily ill-conditioned since  $\Delta t_{\text{crit}}$  depends upon the inverse of the product  $kE$  through a weighting unknown factor  $\chi$  and can be quite small if  $E$  is large;
- conversely, soft highly compressible media may be characterized by a relatively large  $\Delta t_{\text{crit}}$  and hence difficult to solve at early time values;
- if  $\beta \neq 0$  (i.e. compressible fluid), a limiting stiffness of the porous medium exists such that for stiffer systems there is no critical time step;
- if  $\beta = 0$  (i.e. incompressible fluid), a critical time step always exists which is inversely proportional to  $kE$ .

The occurrence of ill-conditioning has been proven using both the convergence rate of Bi-CGSTAB and the conditioning numbers  $L$  and  $D$  with the results in substantial agreement. For the most severe ill-conditioned problems Bi-CGSTAB preconditioned with ILU(0) may fail to converge. For less severe Bi-CGSTAB may still converge but the computational cost to get the solution can increase significantly. Finally, some recommendations are given for remediating at least in part the problem of ill-conditioning.

## Acknowledgements

This work has been partially funded by the Italian MURST project “Metodologie Innovative per il Monitoraggio, la Gestione ed il Controllo Quali-quantitativo delle Acque Sotterranee”, and has been inspired by a research programme which is currently being developed in cooperation with ENI-AGIP S.p.A.

## Appendix A. Mathematical background

A brief summary of the main analytical expressions used in the paper is given below.

Using the classical finite element formulation for elastic continuum (Zienkiewicz and Taylor, 1989; Zienkiewicz, 1991), we can define:

$$\begin{aligned}\boldsymbol{\sigma} &= D\boldsymbol{\epsilon} \\ \boldsymbol{\epsilon} &= LN_u \mathbf{u} = B\mathbf{u} \\ p &= N_p p\end{aligned}$$

and coupling the principle of virtual works with Terzaghi's effective pressure (Terzaghi and Peck, 1967) yields:

$$\left( \int_V B^T D B dV \right) \mathbf{u} - \left( \int_V B^T \mathbf{i} N_p dV \right) \mathbf{p} = \mathbf{f}^u$$

where  $\mathbf{i}$  is the Kronecker  $\delta$  in vectorial form.

The flow equation can be integrated using the classical Galerkin method:

$$\left( \frac{k}{\gamma} \int_V (\nabla N_p) (\nabla N_p)^T dV \right) \mathbf{p} + \left( \int_V N_p^T \mathbf{i}^T B dV \right) \dot{\mathbf{u}} + \left( n\beta \int_V N_p N_p^T dV \right) \dot{\mathbf{p}} = \mathbf{f}^p.$$

Finally:

$$\begin{aligned} K &= \int_V B^T DB dV, \\ Q &= \int_V B^T i N_p dV, \\ H &= \frac{k}{\gamma} \int_V (\nabla N_p) (\nabla N_p)^T dV, \\ P &= n\beta \int_V N_p N_p^T dV. \end{aligned}$$

For more details, see Feronato et al. (2000).

## References

Biot, M.A., 1941. General theory of three-dimensional consolidation. *J. Appl. Phys.* 12 (2), 155–164.

Booker, J.R., Small, J.C., 1975. An investigation of the stability of numerical solutions of Biot's equations of consolidation. *Int. J. Solids Struct.* 11, 907–917.

Chierici, G.L., 1989. *Principi di Ingegneria dei Giacimenti Petroliferi*. Agip, Milano.

Christian, J.J., Boehmer, J.W., 1970. Plain strain consolidation by finite elements. *J. Soil. Mech. Found. Div. ASCE* 96, 1435–1457.

Desai, C.S., 1975. Analysis of consolidation by numerical methods. *Proc. Symp. Recent Develop. Anal. Soil Behavior Appl. Geotech. Struct.* Sidney University of New South Wales.

Duff, I.S., Erisman, A.M., Reid, J.K., 1986. *Direct Methods for Sparse Matrices*. Oxford University Press, Oxford.

Feronato, M., Gambolati, G., Teatini, P., 2000. Total stress and pressure gradient formulations in coupled poroelastic problems. *Proc. Symp. Coupled Phenom. Civil, Mining Petroleum Engng.* Hainan, China.

Gambolati, G., Putti, M., Paniconi, C., 1996. Projection methods for the finite element solution of dual-porosity model in variably saturated porous media. In: Aral, M.M. (Ed.), *Advances in Groundwater Pollution Control and Remediation*. Kluwer, Dordrecht, pp. 97–125.

Gambolati, G., Feronato, M., Teatini, P., Deidda, R., Lecca, G., 2000a. Finite element analysis of land subsidence above depleted reservoirs with the pore pressure gradient and total stress formulations. *Int. J. Numer. Anal. Meth. Geomech.*, in press.

Gambolati, G., Teatini, P., Baú, D., Feronato, M., 2000b. The importance of poroelastic coupling in dynamically active aquifers of the Po river basin, Italy. *Water Resour. Res.* 36 (9), 2443–2459.

Geertsma, J., 1966. Problems of rock mechanics in petroleum production engineering. *Proc. First Cong. Int. Soc. Rock Mechan. Lisbon*, pp. 585–594.

Ghaboussi, J., Wilson, E.L., 1973. Flow of compressible fluid in porous elastic media. *Int. J. Numer. Meth. Engng.* 5, 419–442.

Hwang, C.T., Morgenstern, N.R., Murray, D.T., 1971. On solutions of plane strain consolidation problem by finite element methods. *Can. Geotech. J.* 8, 109–110.

Kershaw, D.S., 1978. The incomplete Cholesky-conjugate gradient method for the iterative solution of systems of linear equations. *J. Comp. Phys.* 26, 43–65.

Lewis, R.W., Schrefler, B.A., 1987. *The Finite Element Method in the Deformation and Consolidation of Porous Media*. Wiley, New York.

Reed, M.B., 1984. An investigation of numerical errors in the analysis of consolidation by finite elements. *Int. J. Numer. Anal. Meth. Geomech.* 8, 243–257.

Saad, Y., 1994. ILUT: a dual threshold incomplete ILU factorization. *Num. Lin. Alg. Appl.* 1, 387–402.

Saad, Y., 1996. *Iterative methods for sparse linear systems*. PWS Publishing, Boston.

Sandhu, R.S., 1976. Finite element analysis of soil consolidation. *Geotech. Engng. Rep. to NSF* 6, The Ohio State University.

Sandhu, R.S., Wilson, E.L., 1969. Finite element analysis of seepage in elastic media. *J. Engng. Mech. Div. ASCE* 95, 641–652.

Sloan, S.W., Abbo, A.J., 1999. Biot consolidation analysis with automatic time stepping and error control. Part 1: theory and implementation. *Int. J. Numer. Anal. Meth. Geomech.* 23, 467–492.

Smith, I.M., Hobbs, R., 1976. Biot analysis of consolidation beneath embankments. *Geotechnique* 26, 149–161.

Terzaghi, K., Peck, R.B., 1967. *Soil Mechanics in Engineering Practice*, 2nd Edition. Wiley, New York.

van der Knaap, W., 1959. Nonlinear behavior of elastic porous media. *Petroleum Trans. AIME* 216, 179–187.

van der Vorst, H.A., 1992. Bi-CGSTAB: a fast and smoothly converging variant of BI-CG for the solution of nonsymmetric linear systems. *SIAM J. Sci. Stat. Comput.* 13, 631–644.

Vermeer, P.A., Verruijt, A., 1981. An accuracy condition for consolidation by finite elements. *Int. J. Numer. Anal. Meth. Geomech.* 5, 1–14.

Verruijt, A., 1969. Elastic storage of aquifers. In: De Wiest, R. (Eds.), *Flow Through Porous Media*. Academic Press, New York, pp. 331–376.

Verruijt, A., 1977. Generation and dissipation of pore water pressure. In: Gudehus, G. (Eds.), *Finite Elements in Geomechanics*. Wiley, London, pp. 293–317.

Westlake, J.R., 1968. *Numerical Matrix Inversion and Solution of Linear Equations*. Wiley, New York.

Zienkiewicz, O.C., 1991. *The Finite Element Method in Engineering Geoscience*, 4th ed. McGraw Hill, London.

Zienkiewicz, O.C., Taylor, R.L., 1989. *The Finite Element Method*, vol. 1, 4th Edition. McGraw Hill, London.